Journal of Thermal Analysis and Calorimetry, Vol. 81 (2005) 243–250

THERMAL AND SPECTRAL PROPERTIES OF Cu(II)-5-HALOGENOSALICYLATES WITH OR WITHOUT NICOTINAMIDE

S. C. Mojumdar[1*], *L. Martiška*[2], *D. Valigura*[2] *and M. Melník*[2]

[1]Institute for Research in Construction, National Research Council of Canada, M-20, 1200 Montreal Road, Ottawa, Ontario K1A 0R6, Canada,
[2]Department of Inorganic Chemistry, Slovak University of Technology, Radlinskeho-9, SK-81237 Bratislava, Slovakia

This paper deals with the preparation and investigation of thermal and spectral properties of the complexes $Cu(5\text{-}ClSal)_2 \cdot 2H_2O$ (**I**), $Cu(5\text{-}BrSal)_2 \cdot 2H_2O$ (**II**), $Cu(5\text{-}ClSal)_2(nia)(H_2O)$ (**III**), $Cu(5\text{-}BrSal)_2(nia)(H_2O)$ (**IV**), and $Cu(5\text{-}ISal)_2(nia)(H_2O)$ (**V**) (where Sal=salicylate, and nia=nicotinamide). TG, DTG, DTA, EPR, IR and electronic spectra have been used to study thermal and spectral properties of the complexes. The chemical composition of the complexes, the solid intermediates and the resultant products of thermolysis have been identified by means of elemental analysis and complexometric titration. Schemes of the decomposition of the complexes are suggested. Heating of the compounds first resulted in the release of water molecules. The thermal stability of these complexes can be ordered in the sequence: **I** <**II** <**IV**=**V**< **III**. The final product of the thermal decomposition was CuO in all cases. IR data suggested a bidentate coordination of carboxylates to Cu(II) in complexes **I**–**II** and bridging ones for complexes **III**–**V**.

Keywords: *copper(II)-5-halogenosalicylate and copper(II)-5-halogenosalicylate-nicotinamide complexes, DTA, EPR, IR, pyrolysis, TG, UV-VIS*

Introduction

The coordination ability of salicylic acid and its derivatives to form complexes with different metal ions is well known [1]. Salicylatocopper(II) complexes are of interest from the chemical and biological points of view. For example copper(II) aspirinate (aspirinate= acetylsalicylate) complexes [2] have been found to be better antiinflammatory agents than aspirin, and have shown some antiulcer activity [3]. The above mentioned complexes have been found to be effective against rheumatoid disorders, and are active in reducing seizure, and in decreasing the rate of tumor growth [2]. Due to the presence of the hydroxyl group, salicylates exhibit more different bonding modes than benzoates [4], e.g. chelating bonding including a deprotonization of phenolato-group, forming salicylato dianion [5]. Structures containing 5-halogensalicylate anion bonded to metal atom are rare [6–10]. Different bonding possibilities of 5-chlorosalicylate anion are well documented in all known structures. The chelating bonding mode of 5-chlorosalicylate with oxygen atoms of hydroxyl and carboxyl group was found in tungsten complex [6]. An asymmetric chelating bonding mode of carboxyl group is shown in the structure of tin complex [7]. The bridging bonding mode of carboxyl group was developed in manganese complexes [8, 9]. The monodentate bonding of carboxyl group was published recently [10] for $[Cu(5\text{-}ClSal)_2(H_2O)_2]$.

The structure of metal-carboxylato complexes as well as the study of the influence of metal and ligand nature on the process of thermal decomposition are of great interest. Therefore, it is not surprising that many authors have investigated metal and ligand nature in coordination compounds of several central atoms and also studied their thermal and spectral properties [11–31]. In our previous papers we described the thermoanalytical properties of Mg(II), Cu(II), Co(II) and Fe(III) complexes with carboxylates, pyridine and/or its derivatives [32–43]. Limited data on structure and thermal decomposition of Cu(II) complexes with halogenosalicylic acids are available [4]. Therefore, this paper describes the preparation of complexes formed by halogenosalicylic acids with Cu(II), and/or nicotinamide along with their thermal and spectral analyses.

Experimental

Preparation of the complexes

Complexes **I** and **II** were prepared according to the published procedure [4] with the exception of the addition

* Author for correspondence: e-mail: subhash.mojumdar@nrc-cnrc.gc.ca

1388–6150/$20.00

Akadémiai Kiadó, Budapest, Hungary
Springer, Dordrecht, The Netherlands

of stoichiometric amount of the appropriate halogenosalicylic acids to the solution of copper acetate in water. The mixtures were stirred with the magnetic stirrer and the precipitation of different colored products occurred. After several days the stable colored products were filtered off, washed with water and dried in air.

All nicotinamide complexes (**III**–**V**) were prepared using a similar procedure as described in [4] by adding a stoichiometric amount of nicotinamide to the water solution of copper acetate. The stoichiometric amount of halogenosalicylic acid was added to the reaction mixture after dissolution of nicotinamide under stirring. The mixtures were stirred for several days, then the products were filtered off, washed with water and dried in air.

Complexometric titration

The complexes (**I**–**V**) and the products and intermediates of thermal decomposition were mineralized by heating in aqueous solution of nitric acid. The residual nitric acid in the clear solutions were neutralized by pastilles of sodium hydroxide and finally the acidity was adjusted just below pH=7 with the dilute solutions of ammonia and/or nitric acid. Thus obtained aqueous solutions were used for titration by the standardized solution of disodium salt of ethylenediaminetetraacetic acid (EDTA) using murexid as indicator.

Thermal analyses

Thermal decompositions of the complexes were conducted using a TA Instruments module. Measurements were carried out between room temperature and 1000°C in an atmosphere of dynamic air at a heating rate of 10°C min^{-1}. The sample mass were 10–20 mg.

Spectral measurements

Electronic spectra in the region 200–1100 nm were measured with a Specord 200 spectrophotometer. IR spectra in the region 4000–200 cm^{-1} were recorded by means of a Nicolet Magna 750 FTIR spectrometer. In both measurements the Nujol suspension technique was used. EPR spectra of powdered samples were recorded at room temperature using a Brucker SRC-200D model of EPR spectrometer.

Results and discussion

Chemical analysis of the compounds

The contents of carbon, nitrogen and hydrogen were determined by elemental analysis and the contents of copper were determined by complexometric titration. The results, given in Table 1 are in good agreement with theoretical expectations.

*Thermal decomposition of the complexes **I**–**V***

The thermal decomposition data of the complexes **I**–**V** are collected in Table 2. The complexes **III**–**V** are thermally more stable than complexes **I** and **II**. Thermal decompositions of the complexes **I**–**V** are multistage processes. The subsequent detachment of the ligands was observed. The final solid product was CuO.

The TG and DTA curves for the decomposition of $Cu(5\text{-}ClSal)_2{\cdot}2H_2O$ (**I**) are shown in Fig. 1. The TG curve indicates that it is thermally stable up to 90°C. Afterwards, the TG curve shows five mass loss steps. The first step between 90 and 145°C is accompanied by 8.15% mass loss (measured from the TG curve by TA instrument software), and is attributed to the dehydration process. The second step took place between 155 and 218°C and is accompanied by 16.00% mass loss. It is attributed, however, to the decomposition of the anhydrous complex to $Cu(Sal)_2$. The third step took place between 218 and 278°C and is accompanied by 17.70% mass loss. It is attributed, however, to the partial decomposition of $Cu(Sal)_2$ to $Cu(Sal)(HCO_3)$. The fourth step took place between 278 and 344°C and is accompanied by 36.15% mass loss. It is attributed, to the decomposition of $Cu(Sal)(HCO_3)$ to $Cu(OH)_2$. The fifth step took place between 344 and 423°C, accompanied by 4.07% mass loss. It is attributed to the elimination of H_2O with the formation of CuO as the final solid product. The thermal decomposition reactions of complexes **I** and **II** can be represented as:

Table 1 Chemical analyses data of the complexes **I**–**V**

Complex	Theoretical/ %				Experimental/%			
	C	H	N	Cu	C	H	N	Cu
$Cu(5\text{-}ClSal)_2{\cdot}2H_2O$ (**I**)	37.98	2.73	–	14.35	38.35	2.76	–	14.44
$Cu(5\text{-}BrSal)_2{\cdot}2H_2O$ (**II**)	31.63	2.28	–	11.95	31.80	2.18	–	11.75
$Cu(5\text{-}ClSal)_2(nia)(H_2O)$ (**III**)	43.93	2.95	5.12	11.62	43.76	2.99	5.04	11.70
$Cu(5\text{-}BrSal)_2(nia)(H_2O)$ (**IV**)	37.79	2.54	4.41	10.00	37.47	2.41	4.25	10.19
$Cu(5\text{-}ISal)_2(nia)(H_2O)$ (**V**)	32.92	2.21	3.84	8.71	32.45	2.12	3.60	8.45

Table 2 Thermal decomposition data of the complexes **I**–**V**

Complex	DTA results			TG results		
	T_{peak}/°C		T_{range}/°C	Mass loss/% Found (Calc.)	Loss of	Composition of residue
$Cu(5\text{-}ClSal)_2\cdot 2H_2O$ (**I**)	120	endo	90–155	8.15 (8.14)	H_2O	$Cu(5\text{–}ClSal)_2$
	175	endo	155–218	16.00 (16.02)	Cl_2	$Cu(Sal)_2$
	248	endo	218–278	17.70 (16.96)	decomp. of Sal	$Cu(Sal)(HCO_3)$
	329	exo	278–344	36.15 (36.84)	decomp. of anions	$Cu(OH)_2$
	392	exo	344–423	4.07 (4.07)	H_2O	CuO
$Cu(5\text{-}BrSal)_2\cdot 2H_2O$ (**II**)	125	endo	85–151	7.15 (6.78)	H_2O	$Cu(5\text{–}BrSal)_2$
	206	endo	151–261	30.05 (30.06)	Br_2	$Cu(Sal)_2$
	306	exo	261–433	14.68 (14.13)	decomp. of Sal	$Cu(Sal)(HCO_3)$
	457	exo	433–559	30.68 (30.12)	decomp. of anions	$Cu(OH)_2$
	585	exo	559–592	3.17 (3.39)	H_2O	CuO
$Cu(5\text{-}ClSal)_2(nia)\cdot(H_2O)$ (**III**)	136	endo	113–203	3.47 (3.29)	H_2O	$Cu(5\text{–}ClSal)_2(nia)$
	239	endo	203–310	62.74 (63.67)	Cl_2, nia, SalH	$Cu(Sal_{-H})$
	387, 501	exo	310–548	25.08 (24.70)	decomp. of dianions	CuO
$Cu(5\text{-}BrSal)_2(nia)\cdot(H_2O)$ (**IV**)	138	endo	112–202	2.82 (2.83)	H_2O	$Cu(5\text{–}BrSal)_2(nia)$
	289	endo	202–446	67.92 (68.75)	Br_2, nia, SalH	$Cu(Sal_{-H})$
	565	exo	446–650	21.98 (21.25)	decomp. of dianion	CuO
$Cu(5\text{-}ISal)_2(nia)\cdot(H_2O)$ (**V**)	130	endo	112–200	2.67 (2.47)	H_2O	$Cu(5\text{–}ISal)_2(nia)$
	243	endo	200–320	52.61 (53.99)	Br_2, nia	$Cu(Sal)_2$
	387, 466	exo	320–500	34.58 (35.11)	decomp. of 2Sal	CuO

$$Cu(5\text{-}XSal)_2\cdot 2H_2O \rightarrow Cu(5\text{-}XSal)_2 + 2H_2O$$

$$Cu(5\text{-}XSal)_2 \rightarrow Cu(Sal)_2 + X_2$$

$$Cu(Sal)_2 \rightarrow Cu(Sal)(HCO_3) + \text{Decomposition products of Sal}$$

$$Cu(Sal)(HCO_3) \rightarrow Cu(OH)_2 + 2CO_2 + \text{Decomposition products of Sal}$$

$$Cu(OH)_2 \rightarrow CuO + H_2O$$

(*X*=Cl or Br in complexes **I** or **II**, respectively)

The DTA curve for complex **I** (Fig. 1) shows three endothermic peaks at 120, 175 and 248°C ascribed to the loss of $2H_2O$, Cl_2 and C_6H_6, respectively, and two exothermic peaks maximized at 329 (very intensive) and 392°C (less intensive) corresponding to the decomposition of $Cu(Sal)(HCO_3)$ and $Cu(OH)_2$, respectively. The DTA results also show the simultaneous formation of CuO.

The TG and DTA curves of $Cu(5\text{-}BrSal)_2\cdot 2H_2O$ (**II**) are presented in Fig. 2. The TG curve for this complex indicates that it is thermally stable up to 85°C, where the dehydration process commences. This is followed by another four mass loss steps. The second step between 151 and 261°C is accompanied by 30.05% mass loss and attributed to the decomposition of the anhydrous complex to $Cu(Sal)_2$. The third step between 261 and 433°C is accompanied by 14.68% mass loss. It is attributed to the decomposition of $Cu(Sal)_2$ to $Cu(Sal)(HCO_3)$. The fourth step took place between 433 and 559°C, accompanied by 30.12% mass loss. It is attributed to the decomposition of $Cu(Sal)(HCO_3)$ to $Cu(OH)_2$. The fifth step took place between 559 and 592°C and is accompanied by 3.39% mass loss. It is attributed to the elimination of H_2O with the simultaneous formation of CuO as the final solid product.

The DTA curve for complex **II** (Fig. 2) shows two endothermic peaks at 125 and 206°C attributed to

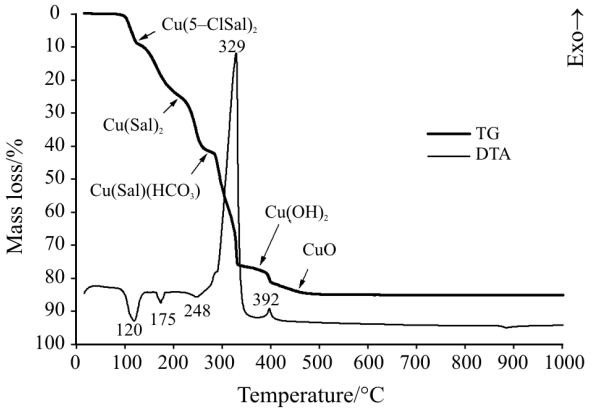

Fig. 1 TG and DTA curves of $Cu(5\text{-}ClSal)_2\cdot 2H_2O$ (**I**)

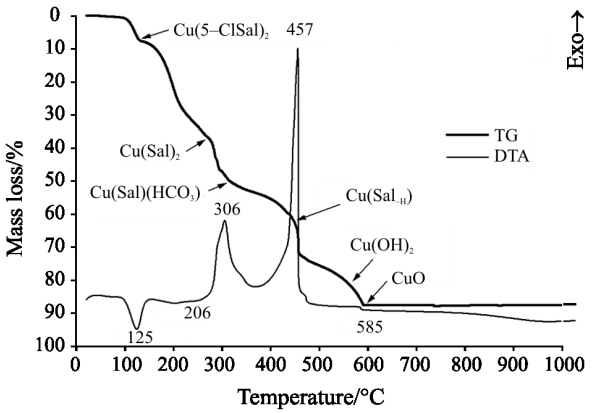

Fig. 2 TG and DTA curves of $Cu(5\text{-}BrSal)_2{\cdot}2H_2O$ (**II**)

the loss of $2H_2O$ and Br_2, respectively, and three exothermic peaks maximized at 306, 457, and 585°C corresponding to the decomposition of $Cu(Sal)_2$, $Cu(Sal)(HCO_3)$ and $Cu(OH)_2$, respectively with the simultaneous formation of CuO.

The tentative intermediate decomposition products of complexes **I** and **II** are similar to the thermal decomposition of $Cu(5\text{-}ISal)_2{\cdot}2H_2O$, published recently [4] with the exception of the formation of $Cu(Sal)(HCO_3)$ and $Cu(OH)_2$.

The TG and DTA curves for the decomposition of $Cu(5\text{-}ClSal)_2(nia)(H_2O)$ (**III**) are shown in Fig. 3. The TG curve indicates that it is thermally more stable (up to 113°C) than complex **I**. Afterwards, the TG curve shows three main mass loss steps. The first step between 113 and 203°C is accompanied by 3.47% mass loss. It is attributed to the dehydration process. The second step between 203 and 310°C is accompanied by 60.38% mass loss. This step is attributed to the loss of nicotinamide, Cl_2 and salicylic acid and the residue could be assigned to $Cu(Sal_{-H})$ (where Sal_{-H} represents salicylate dianion known for some salicylato complexes [5]). The third step took place between 310 and 548°C and is accompanied by 24.70% mass loss. It is attributed to the loss of organic moiety and to the decomposition of $Cu(Sal_{-H})$ to CuO. The thermal reaction of complex **III**–**V** can be represented as:

$$Cu(5\text{-}XSal)_2(nia)(H_2O) \rightarrow Cu(5\text{-}XSal)_2(nia)+H_2O$$

$$Cu(5\text{-}X\text{Sal})_2(nia)\rightarrow Cu(Sal_{-H})+nia+X_2+ \\ +\text{Decomposition products of Sal}$$

$$Cu(Sal_{-H})\rightarrow CuO+\text{Decomposition products of } Sal_{-H}$$

(*X*=Cl, Br or I in complexes **I**, **II** or **III**, respectively)

The DTA curve for complex **III** (Fig. 3) shows two endothermic peaks at 136 and 239°C corresponding to the loss of H_2O and formation of $Cu(Sal_{-H})$, respectively, and a broad exothermic peak with two maxima of different intensity at 387 and 501°C attributed to the decomposition reaction of $Cu(Sal_{-H})$ with the simultaneous formation of CuO.

The TG and DTA curves for the decomposition of $Cu(5\text{-}BrSal)_2(nia)(H_2O)$ (**IV**) are shown in Fig. 4. The TG curve indicates that it is thermally more stable (up to 112°C) than complex **II**. Afterwards, the TG curve shows three main mass loss steps. The first step between 112 and 202°C is accompanied by 2.82% mass loss. It is attributed to the dehydration process. The second step between 202 and 446°C is accompanied by 65.92% mass loss. This step is attributed to the loss of nicotinamide, Br_2 and salicylic acid and the residue could be assigned to $Cu(Sal_{-H})$ (where Sal_{-H} represents salicylate dianion) [5]. The third step took place between 446 and 650°C and is accompanied by 21.98% mass loss. It is attributed to the loss of organic moiety and decomposition of $Cu(Sal_{-H})$ to CuO as the final solid product.

The DTA curve for complex **IV** (Fig. 4) shows two endothermic peaks at 138°C and 289°C, attributed to the loss of (H_2O and Br_2, nicotinamide and salicylic acid), respectively and an exothermic peak at 565°C attributed to the decomposition reaction of $Cu(Sal_{-H})$ to CuO.

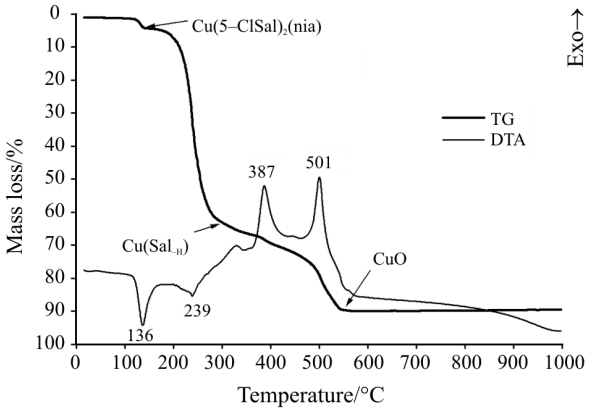

Fig. 3 TG and DTA curves of $Cu(5\text{-}ClSal)_2(nia)(H_2O)$ (**III**)

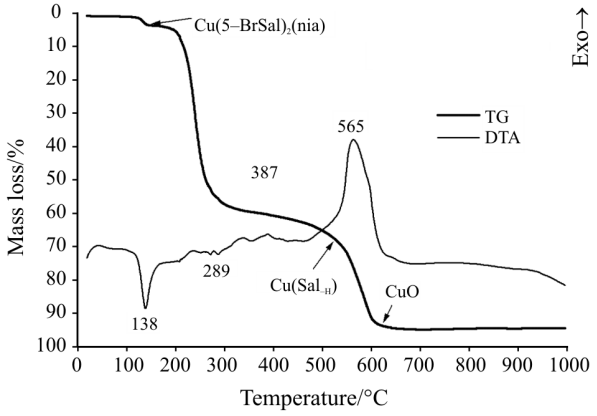

Fig. 4 TG and DTA curves of $Cu(5\text{-}BrSal)_2(nia)(H_2O)$ (**IV**)

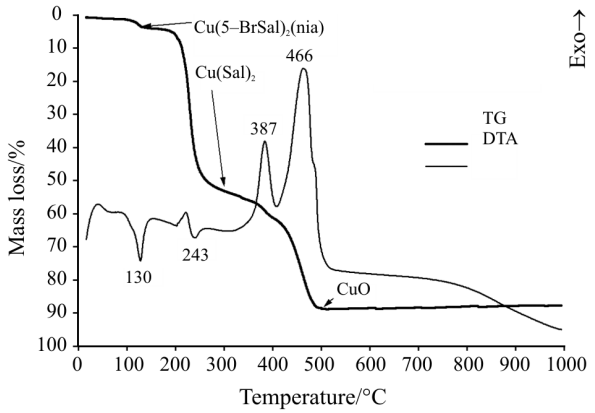

Fig. 5 TG and DTA curves of $Cu(5\text{-}ISal)_2(nia)(H_2O)$ (**V**)

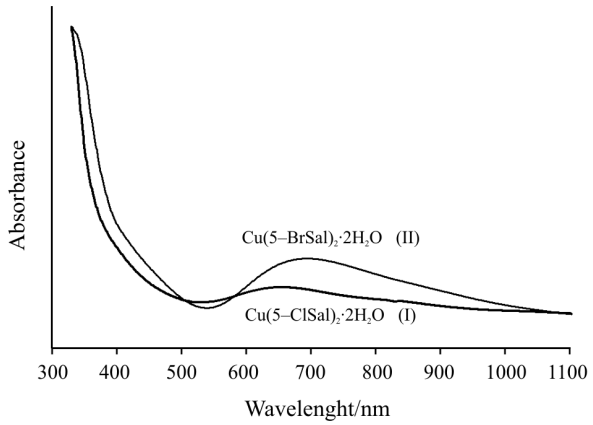

Fig. 6 Electronic spectra of complexes **I** and **II**

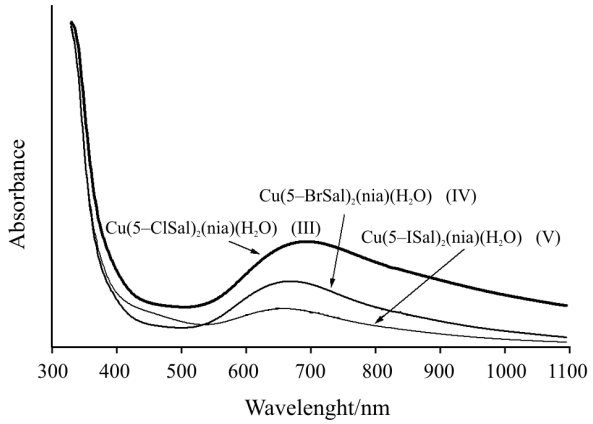

Fig. 7 Electronic spectra of complexes **III**–**V**

The TG and DTA curves for the decomposition of $Cu(5\text{-}ISal)_2(nia)(H_2O)$ (**V**) are presented in Fig. 5. The TG curve for this compound indicates that it is thermally more stable (up to 112°C) than the corresponding complex, published in [4]. Afterwards, the TG curve shows three main mass loss steps. The first step between 112 and 200°C is accompanied by 2.67% mass loss. It is attributed to the dehydration process. The second step between 200 and 320°C is accompanied by 51.52% mass loss. This step is attributed to the loss of nicotinamide and I_2, and the residue could be assigned to $Cu(Sal)_2$. Thus, the thermal decomposition of this complex exhibits some differences in comparison to complexes **III** and **IV**. The third step took place between 320 and 500°C and is accompanied by 34.58% mass loss. It is attributed to the decomposition of $Cu(Sal)_2$ and to the formation of copper oxide as the final solid product.

The DTA curve for complex **V** (Fig. 5) shows two endothermic peaks at 130 and 243°C ascribed to the elimination of H_2O and nia respectively and a broad exothermic peak with two maxima at 387 and 466°C corresponding to the decomposition reaction of $Cu(Sal)_2$ with the simultaneous formation of CuO.

The stoichiometry of thermal decomposition can also be influenced by the changes of experimental conditions, origin and preparation history. Though the final product of the thermal decomposition of complexes **I**–**V** is CuO, but the origin and preparation history are different. Due to this reason, CuO was formed in different temperature as the final decomposition of different complexes.

Electronic spectroscopy

The compounds $Cu(5\text{-}ClSal)_2{\cdot}2H_2O$ (**I**) $Cu(5\text{-}BrSal)_2{\cdot}2H_2O$ (**II**) are of light green color, the compounds $Cu(5\text{-}ClSal)_2(nia)(H_2O)$ (**III**), $Cu(5\text{-}BrSal)_2(nia)(H_2O)$ (**IV**) are of light blue color, the $Cu(5\text{-}ISal)_2(nia)(H_2O)$ (**V**) complex is of light turquoise-blue color. Electronic Spectra of complexes **I**–**V** are presented in Figs 6–7. All studied compounds exhibit weak and very broad and asymmetric $d \rightarrow d$ transition bands with maxima between 650 and 700 nm (Table 3). All compounds exhibit weak and unresolved shoulders at lower energy side that are consistent with proposed pseudo–octahedral structure that was structurally confirmed in X-ray structure determination of the $Cu(5\text{-}ClSal)_2{\cdot}2H_2O$ structure [10].

The UV absorptions of **I**–**V** could be assigned to π–π^* transitions of the aromatic system of salicylato anions bonded to copper(II) atom. All five compounds exhibit shoulders between 380–480 nm that could be assigned as charge–transfer and thus attributed to the characteristic deformation of interaction [10].

EPR spectroscopy

EPR spectra of the complexes **I**–**V** at room temperature are presented in Figs 8–9. EPR spectra of the compounds **I**–**V** showed the typical absorption bands of monomeric species and all of them are of axial symmetry. The spectra can be interpreted without hyperfine structure resolved by using a spin

Table 3 Selected electronic and EPR spectral data

Complex	Electronic spectra[a]	$g_\perp$	g_{II}	g_{av}	G
$Cu(5\text{-}ClSal)_2{\cdot}2H_2O$ (**I**)	400sh, 653br	2.040	2.320	2.133	8.0
$Cu(5\text{-}BrSal)_2{\cdot}2H_2O$ (**II**)	420sh, 680br	2.049	2.310	2.136	6.3
$Cu(5\text{-}ClSal)_2(nia)(H_2O)$ (**III**)	400sh, 697br	2.040	2.310	2.130	7.8
$Cu(5\text{-}BrSal)_2(nia)(H_2O)$ (**IV**)	400sh, 673br	2.050	2.320	2.140	6.4
$Cu(5\text{-}ISal)_2(nia)(H_2O)$ (**V**)	450sh, 680br	2.034	2.310	2.126	9.1

[a] CT band; $d\rightarrow d$ band(s), all values are in nm. sh = shoulder, br - broad

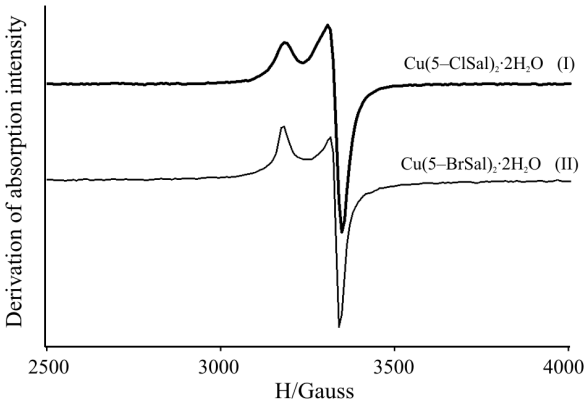

Fig. 8 EPR spectra of complexes **I** and **II**

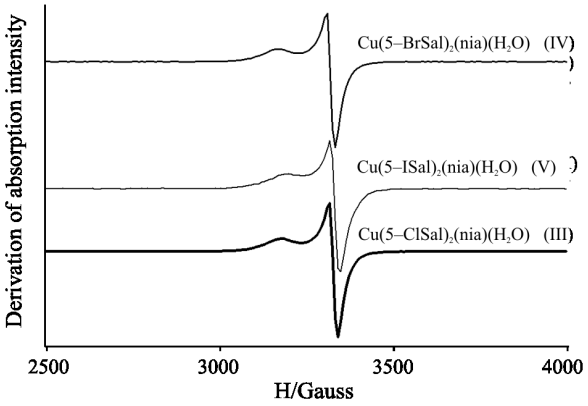

Fig. 9 EPR spectra of complexes **III**–**V**

Hamiltonian for axial symmetry. The obtained g values ($g_\perp$, g_{II} and g_{av}) are shown in Table 3 together with a G parameter values and are consistent with proposed pseudo-octahedral symmetry. The g values (the lowest value g>2.04 and the value of parameter G>4) are typical for an elongated octahedral coordination about Cu(II) atom with local tetragonal axes aligned parallel, and with $d^2_{x-y^2}$ ground state.

IR spectroscopy

The most important infrared spectral data of compounds **I**–**V** are reported in Table 4. The IR spectra of compounds **I**–**V** showed broad absorption bands between 3500–3200 cm^{-1}. These frequencies correspond to the assymmetric and symmetric OH stretching [44]. These bands together with the bands assigned to ρ(HOH) vibration clearly confirm the presence of water in these compounds. In this region, the complexes **III**–**V** shows two additional sharper peaks that could be assigned to the symmetric and assymmetric NH vibrations of nicotinamide. This fact together with a small shift of aromatic CN vibrations are clear confirmations of nicotinamide coordination through pyridine nitrogen atom to Cu(II).

Carboxylate ions can coordinate to metal ions in a number of ways such as unidentate, bidentate (chelating) or bridging. The analysis of COO^- group bands allowed for the determination of the parameter $\Delta_{COO}=\nu COO^-(as)-COO^-(s)$. The magnitude of Δ_{COO} has been used by Nakamoto [44] as a criterion of the

Table 4 Infrared spectral data (4000–200 cm^{-1}) of complexes **I**–**V**

Assignments	**I**	**II**	**III**	**IV**	**V**
ν(NH)	–	–	3419, 3285	3415, 3290	3415, 3280
ν(OH)	3319, 3197	3340, 3216	3321, 3204	3321, 3203	3315, 3204
ν(C=O)	–	–	1681	1678	1673
$\nu_{as}(COO^-)$	1599, 1574	1590, 1547	1600	1600	1599
$\nu_s(COO^-)$	1473, 1431	1469, 1450	1429	1428	1426
ΔCOO	126, 143	121. 97	171	172	173
ν(CN)	–	–	1597	1598	1599
ρ(HOH)	817, 798	818, 800	829, 808	823, 808	821, 808

as=Assymmetric and s=Symmetric

way by which carboxylates bind to metal ions. From the IR spectra, the calculated values of Δ_{COO} for complexes **I** and **II** were close to 100 cm^{-1}. These values are in good agreement with literature data for the chelating mode of bonding of salicylate anions [40], which are similar to those found for *quasi*-chelating bonding mode in $Cu(5\text{-}ClSal)_2 \cdot 2H_2O$ structure [10]. The doublet structure of COO^- group bands is understandable on the $Cu(5\text{-}ClSal)_2 \cdot 2H_2O$ structural [10] data, where two nonequivalent salicylate anions were observed. The calculated values of Δ_{COO} for complexes **III**–**V** were close to 170 cm^{-1}. These values are within the region typical for the bridging bonding mode of carboxylate group [44].

Conclusions

All complexes **I**–**V** are hydrated and showed reasonable stability in air. They exhibit low solubility in water, moderate solubility in ethanol, and high solubility in methanol and dimethylsulfoxide. The decompositions of these compounds were initiated by the elimination of water. Then the decomposition of halogenosalicylato anions occurred (on the TG curves) in one or more steps. The thermal stability of the complexes can be ordered in the sequence: **I<II<IV=V<III**. The results revealed that the final product in the thermal degradation experiments of complexes **I**–**V** was CuO. The stoichiometry of thermal decomposition can also be influenced by the changes of experimental conditions, origin and preparation history [45, 46]. By means of spectral analyses, the structures of the compounds have been studied. Infrared spectral data suggested that one oxygen atom of carboxylate ions is used in the coordination to Cu(II) and the other one is used in the formation of asymmetrical hydrogen bond bridges similar to those found in the $Cu(5\text{-}ClSal)_2 \cdot 2H_2O$ structure [10]. EPR data suggested an elongated axial symmetry of their coordination polyhedra. Without X-ray analysis, no definite structure can be described for the different components. However, spectroscopic and analytical data together with the available thermal analysis techniques enabled us to predict the structures of these complexes.

Acknowledgements

We wish to thank the Ministry of Education of the Slovak Republic, VEGA 1/9251/02 and Natural Research Council of Canada (NRC) for financial support .

References

1 M. Melník, J. Inorg. Nucl. Chem., 40 (1978) 463.
2 F. T. Greenaway, A. Pezeshk, A. W. Cordes, M. C. Noble and J. R. J. Sorenson, Inorg. Chim. Acta, 93 (1984) 67, and references therein.
3 J. R. J. Sorenson, Progr. Med. Chem., 15 (1978) 211.
4 S. C. Mojumdar, L. Martiška, D. Valigura and M. Melník, J. Therm. Anal. Cal., 74 (2003) 905.
5 A. Pajunen and S. Pajunen, Cryst. Struct. Commun., 11 (1982) 427.
6 T. E. Baroni, J. A. Heppert, R. R. Hodel, R. P. Kingsborough, M. D. Morton, A. L. Rheingold and G. P. A. Yap, Organometallics, 15 (1996) 4872.
7 M. Gielen, M. Boualam, B. Mahieu and E. R. T. Tiekink, Appl. Organomet. Chem., 8 (1994) 19.
8 D. A. Malamatari, P. Hitou, A. G. Hatzidimitriou, F. E. Inscore, A. Gourdon, M. L. Kirk and D. P. Kessissoglou, Inorg. Chem., 34 (1995) 2493.
9 V. Tangoulis, D. A. Malamatari, K. Soulti, V. Stergiou, C. P. Raptopoulou, A. Terzis, A. Kabanos and D. P. Kessissoglou, Inorg. Chem., 35 (1996) 4974.
10 M. Melník, M. Koman, J. Moncol' and T. Glowiak, J. Coord. Chem., 53 (2001) 173.
11 D. Czakis-Sulikowska, A. Czylkowska and A. Malinowska, J. Therm. Anal. Cal., 67 (2002) 667.
12 E. Jóna, M. Kubranová, P. Šimon and J. Mroziński, J. Thermal Anal., 46 (1996) 1325.
13 E. Jóna, A. Sirota, P. Šimon and M. Kubranová, Thermochim. Acta, 258 (1995) 161.
14 W. Linert, M. Enamullah, V. Gutmann and R. F. Jameson, Monatsh. Chem., 125 (1994) 661.
15 K. Kundu and M. A. H. Miah, Jahangirnagar Univ. J. Sci., 19 (1995) 49.
16 M. Enamullah and W. Linert, J. Coord. Chem., 35 (1995) 325.
17 R. N. Patel and K. B. Pandeya, Synth. React. Inorg. Met.-Org. Chem., 28 (1998) 23.
18 J. S. Skoršepa, K. Györyová and M. Melník, J. Thermal Anal., 44 (1995) 169.
19 R. N. Patel and K. B. Pandeya, J. Inorg. Biochem., 72 (1998) 109.
20 E. Jóna, M. Hvastijová and J. Kohout, J. Thermal Anal., 41 (1994) 161.
21 G. D'ascenzo, U. B. Ceipidor, E. Cardarelli and A. D. Magri, Thermochim. Acta, 13 (1975) 449
22 E. A. Ukraintseva, V. A. Logvinenko, D. V. Soldatov and T. A. Chingina, J. Therm. Anal. Cal., 75 (2004) 337.
23 B. R. Srinivasan and S. C. Sawant, Thermochim. Acta, 402 (2003) 45.
24 D. Czakis-Sulikowska and A. Czylkowska, J. Therm. Anal. Cal., 71 (2003) 395.
25 E. Jóna and M. Jamnický, J. Thermal Anal., 27 (1983) 359.
26 M. Melník, M. Koman and T. Glowiak, Polyhedron, 17 (1998) 1767.
27 E. Jóna, T. Šramko and J. Gažo, J. Thermal Anal., 16 (1979) 213.
28 A. Krutošíková, B. Mitasová, E. Jóna and M. Bobošíková, Chem. Papers, 55 (2001) 290.
29 M. Melník, I. Potočnak, L. Macášková and D. Mikloš, Polyhedron, 15 (1996) 2159 and refs therein.

30 S. Cakir, I. Bulut, E. Bicer, E. Coskun and O. Cakir, J. Electroanal. Chem., 511 (2001) 94.
31 D. Czakis-Sulikowska, A. Czylkowska and A. Malinowska, J. Therm. Anal. Cal., 65 (2001) 505.
32 S. C. Mojumdar, M. Melník and E. Jóna, J. Anal. Appl. Pyrolysis, 46 (1998) 147.
33 S. C. Mojumdar, M. Melník and E. Jóna, Polish J. Chem., 73 (1999) 293.
34 S. C. Mojumdar, M. Valko and M. Melník, Chem. Papers, 52 (1998) 650.
35 S. C. Mojumdar, M. Melník and M. Valko, Polish J. Chem., 73 (1999) 457.
36 S. C. Mojumdar, M. Melník and E. Jóna, J. Anal. Appl. Pyrol., 48 (1999) 111.
37 S. C. Mojumdar, J. Therm. Anal. Cal., 64 (2001) 629.
38 S. C. Mojumdar, D. Hudecová and M. Melník, Polish J. Chem., 73 (1999) 759.
39 S. C. Mojumdar, M. Melník and E. Jóna, J. Therm. Anal. Cal., 56 (1999) 533.
40 S. C. Mojumdar, M. Melník and E. Jóna, J. Therm. Anal. Cal., 56 (1999) 541.
41 S. C. Mojumdar, M. Melník and E. Jóna, J. Anal. Appl. Pyrolysis, 53 (2000) 149.
42 S. C. Mojumdar, K. Lebrušková and D. Valigura, Chem. Papers, 57 (2003) 245.
43 S. C. Mojumdar, I. Ondrejkovičová, L. Neviďanská and M. Melník, J. Anal. Appl. Pyrolysis, 64 (2002) 59.
44 K. Nakamoto, Infrared and Raman Spectra of Inorganic and Coordination Compounds, Wiley, New York, (1986), p. 283.
45 T. Šramko, G. Liptay and E. Jóna, J. Thermal Anal., 12 (1977) 217.
46 Y. Masuda, Thermochim. Acta, 39 (1980) 235.

DOI: 10.1007/s10973-005-7003-2